International Journal of Thermophysics, Vol. 17, No. 5, 1996

Nanosecond Laser-Induced Thermal Evaporation of Silicon Carbide[1]

R. Reitano[2, 3] and P. Baeri[2]

Excimer (XeCl) laser pulses, 15 ns in duration and with fluences up to 10 $J \cdot cm^{-2}$, have been employed to induce melting and evaporation of 6H–SiC thin layers in vacuum. Sample surface modification in the nanosecond time scale have been monitorized *in situ* by optical probing. Eventually, the ablation product was collected on silicon single-crystal substrates placed in front of the SiC target. Modeling of the heating and the thermal evaporation processes resulted in estimation of surface temperatures as high as 10,000 K, evaporation rates of the order of 10^{25} molecules $\cdot cm^{-2} \cdot s^{-1}$ and recoil pressures of the order of 1 GPa. Comparison with experiments showed that the simple mechanism of purely thermal evaporation is able to describe the process of particle removal from a surface by short laser pulses only in the low-energy density range. Above a certain threshold the model breaks down and other mechanisms have to be considered.

KEY WORDS: evaporation; laser pulse; melting; silicon carbide.

1. INTRODUCTION

Pulsed laser deposition of silicon carbide (SiC) has been demonstrated to be a promising tool to obtain both amorphous and crystalline films [1, 2] or even epytaxial films on silicon substrates [3].

Silicon carbide is a compound that can be used in extremely harsh environments because of its thermal, chemical, and mechanical stability.

[1] Paper presented at the Fourth International Workshop on Subsecond Thermophysics, June 27–29, 1995, Köln, Germany.

[2] Dipartimento di Fisica, Universita di Catania, Corso Italia 57, I-95129 Catania, Italy.

[3] To whom correspondence should be addressed.

0195-928X/96/0900-1079$09.50/0

Moreover, as a wide band-gap semiconductor, it is of great interest for electronic and optoelectronic applications.

In contrast with the chemical vapor deposition method [4], SiC deposited by pulsed laser deposition (PLD) requires a much lower substrate temperature, and being a high vacuum process, contamination is marginal.

Although the results reported in the literature have shown that PLD deposited films present a good adhesion, morphology, and stoichiometry, the necessary improvements in their qualities need more investigation on the ablation process itself since a correlation may exist between the film structure and the deposition procedure.

In the present work we have measured the ablation rate of SiC induced by 15-ns XeCl laser pulses in a wide range of laser fluence, from just above the melting threshold up to 10 $J \cdot cm^{-2}$. We show that three regimes of ablation are obtained, depending on the laser fluence. Modeling of the laser-induced heating and melting can give important insights on the mechanism of ablation in the low fluence regime, where thermal evaporation occurs. A thermodynamic interpretation of the onset of strong ablation rates and of the formation of a dense plasma in front of the irradiated target would be of great importance for the understanding of both the ablation process and the properties of the material under study.

2. EXPERIMENTS

XeCl laser pulses, 15 ns in duration, were focused on a 6H–α SiC target in vacuum (10^{-6} Torr) at a 45° angle of incidence. The laser spot size was about 1.5×0.3 mm, with a gaussian profile along the smaller dimension and almost flat in the larger one. A CW argon laser beam ($\lambda =$ 488 nm) was focused on the center of the XeCl laser spot and the transient reflectivity signal was monitored by a fast p–i–n photodiode.

Silicon substrates were placed close to the target tilted 45° with respect to the target normal so that the material emitted from 0 to 90° from the normal to the target surface could be collected. The average target–substrate distance was about 2 cm.

The ablation rate (emitted material per laser pulse) was evaluated from the depth of the crater created by the incoming radiation, measured by optical microscopy. Alternatively, we estimated the amount of emitted material by measuring the amount of material deposited onto the substrate, integrating the thickness profile of the deposited films over the whole solid angle of emission and assuming a sticking coefficient equal to one. The deposit was analyzed by 2-MeV He^+ Rutherford backscattering spectrometry (RBS) and optical microscopy.

3. RESULTS AND DISCUSSION

During laser heating of the SiC target above a certain threshold energy density, a large change in reflectivity was observed. The time duration of the high-reflectivity phase increased with increasing energy density (see Fig. 1), exhibiting the same behavior as silicon and other semiconductors. We were able to define a threshold for the onset of melting at a fluence of $1 \pm 0.05\ \mathrm{J \cdot cm^{-2}}$. It is well-known that laser-induced melting and solidification can be modeled by standard heat flow calculations [5] with a source term given by the absorption of the laser radiation. These calculations have proved to be quite accurate if the optical and thermal parameters of the irradiated material are known with enough accuracy.

In the case of SiC, almost all the parameters needed for the calculations (thermal conductivity, melting temperature, enthalpy, etc.) are known or can be derived from the thermodynamical data tables [6]. The only free parameter in our calculations was the reflectivity of the liquid at a 308-nm wavelength; it was set to 0.5, the value that gives the best agreement with the measured melt duration as function of laser fluence. The result of the calculations is shown in Fig. 1 as a solid line.

The good agreement between the calculations and the experimental data allows us to use the computed temperature profiles in the modelling of the laser induced evaporation. As an example of our calculations, in

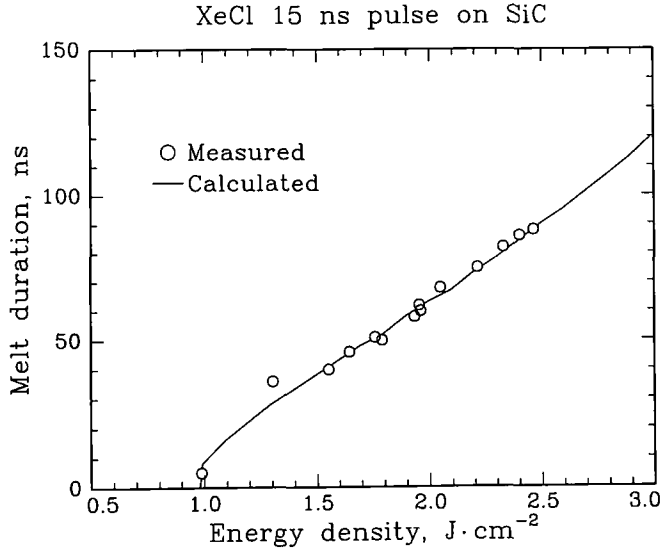

Fig. 1. Melt duration vs laser fluence. (O) Experimental data; (——) heat flow calculations (see text for details.

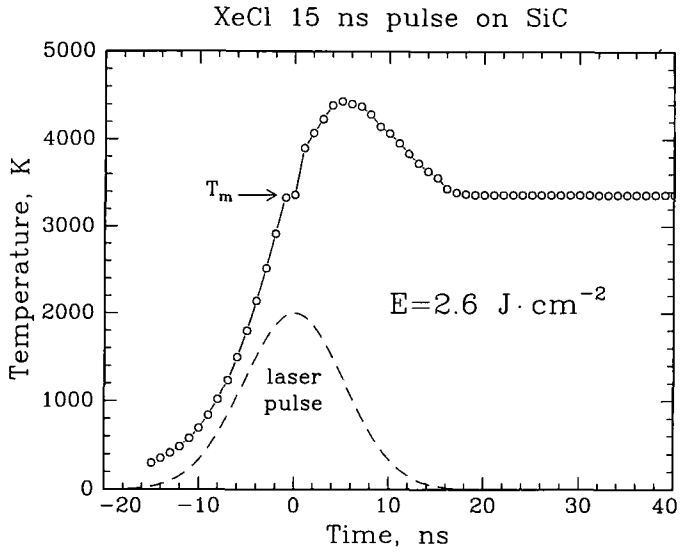

Fig. 2. Calculated surface temperature vs time profile for a laser fluence of 2.6 J · cm^{-2}.

Fig. 2 the computed surface temperature vs time is reported for a 2.6 J · cm^{-2} laser pulse irradiation. After reaching the SiC melting point at ~3200 K, the surface temperature increases to a maximum value of ~5000 K at the peak of the laser pulse and then decreases to the melting point; it remains constant for about 60 ns, until the solidification process is completed.

From these calculations, the time duration of the surface melting and the amount of evaporated material (as shown later) can be calculated.

In Fig. 3, we report the measured ablation rate as a function of the laser fluence. Data obtained from the evaluation of the crater depth are shown as circles, while triangles are used for data obtained by measuring the amount of deposited material. The two methods are in good agreement. The ablation rate shows a well-defined threshold around 1.9 J · cm^{-2} and a sharp increase up to about 600 Å · pulse^{-1} at ~3 J · cm^{-2}; above this fluence the ablation rate remains constant. This behavior is quite similar for many different materials and it is typical of the ablation process. The saturation can be explained by the absorption of the plasma formed in front of the target surface, which prevents the laser light from reaching the surface.

The same data are shown in Fig. 4 on a logarithmic scale. As is clear from the figure, sizable, though very small, ablation is present even below

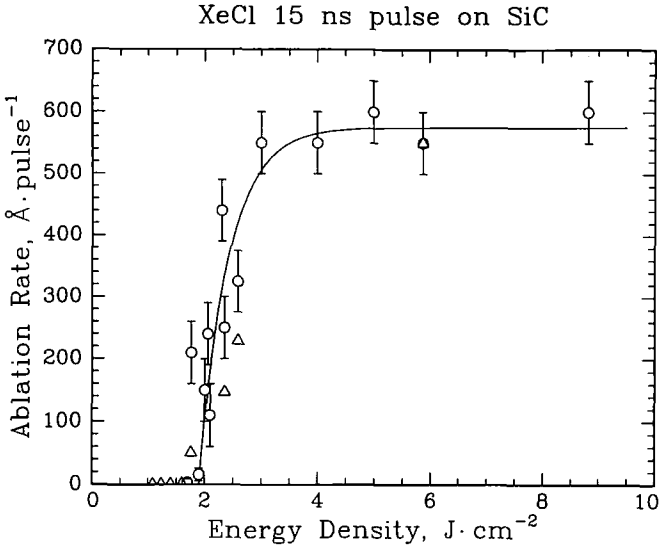

Fig. 3. Ablation rate of 6H-α SiC as a function of laser fluence. (○) Data from material removal. (△) Data from deposited material.

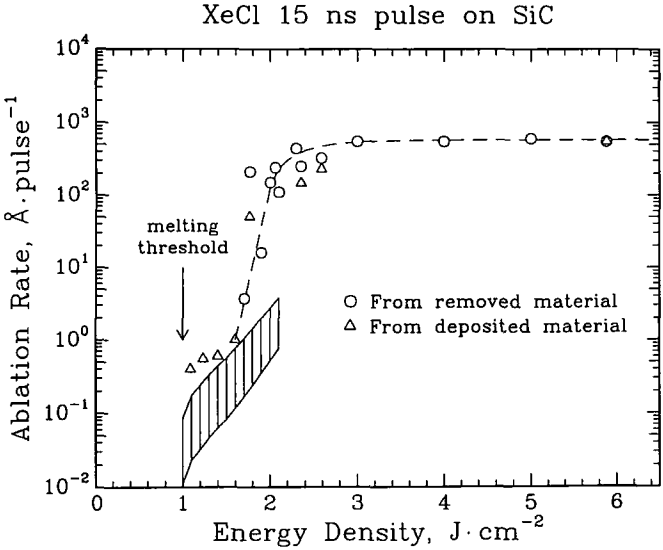

Fig. 4. Same as Fig. 3, on a logarithmic scale. The hatched region is the range of variability of the calculated thermal evaporation as detailed in the text. The dashed line is drawn to guide the eye.

what we call the ablation threshold. Three regions may be identified: just above the melting threshold and up to $1.6\,J \cdot cm^{-2}$ the ablation rate is of the order of a few tenths of an angstrom per pulse and increases slowly with laser fluence; in the range between 1.6 and $2.2\,J \cdot cm^{-2}$ the ablation rate increases dramatically from ~ 1 to $\sim 600\,Å \cdot pulse^{-1}$, and at higher energy density the ablation rate remains constant at this last value.

We now focus our attention on the low-fluence regime, from the melting threshold up to the onset of strong ablation, i.e., before the formation of a dense plasma. Indeed, the presence of plasma alters the process significantly; the gas dynamics and the interaction of the highly excited plasma with the surface and with the incoming light need to be considered. These much more complicated processes are outside the scope of this work.

We have calculated the amount of evaporated material per pulse as a function of the laser fluence by first modeling the surface heating and melting as described above and then calculating the evaporation rate weighted by the surface temperature vs time profile and integrating over time. The evaporation rate as function of temperature [G(T)] is given by

$$G(T) \propto p_v(T) \left(\frac{M}{T}\right)^{1/2} \tag{1}$$

where p_v is the vapor pressure, M the molecular weight, and T the temperature. The vapor pressure can be calculated from the thermodynamic functions. At a given temperature, p_v is given by the pressure at which the free energies of the liquid and the gas are equal. We assumed $\partial V/\partial p = 0$ for the liquid throughout.

For the solid and the gas we used the values reported in the JANAF tables [6]. Not much is known about the liquid phase; some uncertainty is present even on the concentration of the peritectic point, which in turns reflects on the Gibbs free energy of the liquid; the heat of vaporization varies accordingly.

The results of the calculation are shown in Fig. 4 as the hatched area. The two limits of this area correspond to the fit of the two phase diagrams reported in the literature [7, 8], from which two different values of the enthalpy of evaporation ($\Delta H_e = 490\,kJ \cdot mol^{-1}$ and $\Delta H_e = 530\,kJ \cdot mol^{-1}$) can be derived.

It is worth notice that the data on ablation rate below $\sim 1.6\,J \cdot cm^{-2}$ are in good agreement with the calculated thermal evaporation, making this process quite likely to occur. At higher fluences some mechanism, other than the pure thermal evaporation predicted by Eq. (1), arises. A mechanism based on the liquid–gas transition at the critical point has been proposed [9]. At low laser fluence, i.e., before the formation of plasma, the

particles leaving the surface with their own velocity exert a pressure on the liquid; also, the vapor in front of the surface gives another contribution to the pressure on the liquid phase. If the plasma is not dense enough to shield the laser radiation, the temperature of the liquid may rise to a level well above the melting point. A point may be reached where the temperature and the pressure reach their critical value; at this point the liquid transforms with zero enthalpy of evaporation to a highly compressed vapor phase and expands promptly.

The pressure in the liquid can be calculated from the relation $p_l \sim p_g + \rho_g u v_{lg}$, where p is the pressure, ρ_v the density, u the plasma expansion velocity (assumed to be equal to the sonic velocity), and v_{lg} the liquid–gas interface velocity; the subscripts l and g refer to liquid and vapor, respectively. In the low-fluence regime, the second term is dominant; on increasing fluence p_g becomes more and more important. In Fig. 5 the calculated pressure as function of laser fluence is shown.

Assuming the ablation threshold to be around $2\ J \cdot cm^{-2}$, we can then estimate the critical temperature from the heat flow calculations and the critical pressure from the relation above; the results place the critical point of silicon carbide around $T_c \sim 5000$ K and $p_c \sim 100$ MPa.

RBS analysis of the deposited target revealed that films of good stoichiometry were deposited. We obtained films several hundred nanometers thick for the irradiation at the higher fluences ($>2\ J \cdot cm^{-2}$) using a number of

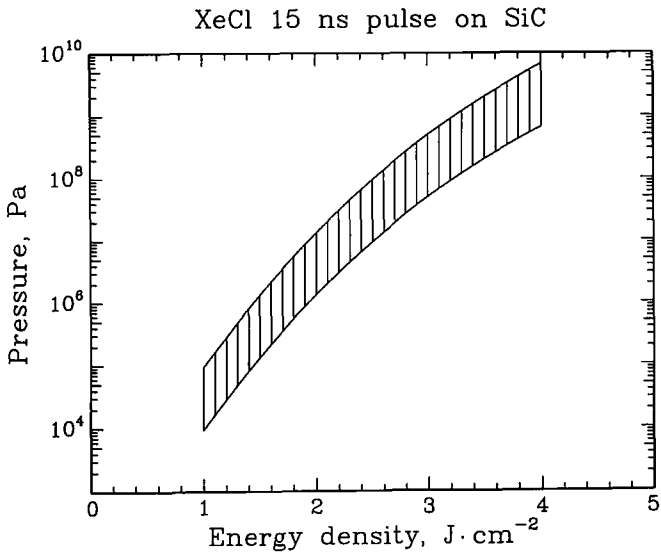

Fig. 5. Calculated liquid pressure as a function of laser fluence.

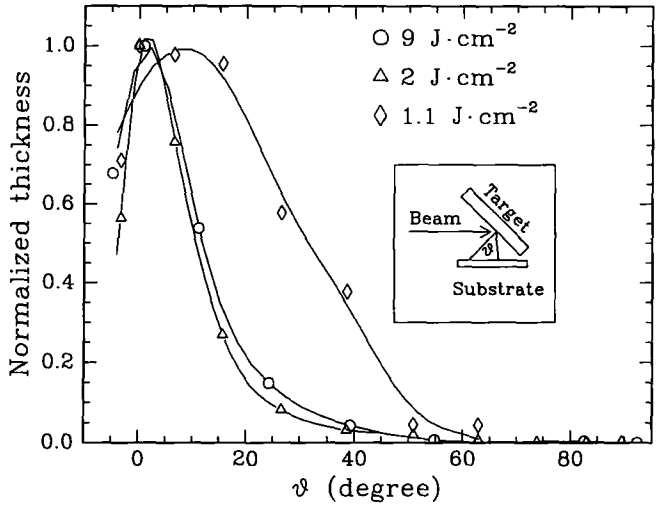

Fig. 6. Normalized thickness of the deposited films as a function of the emission angle ϑ as defined in the inset for three laser fluences. (○) $E = 9\ \mathrm{J \cdot cm^{-2}}$; (△) $E = 2\ \mathrm{J \cdot cm^{-2}}$; (◇) $E = 1.1\ \mathrm{J \cdot cm^{-2}}$.

laser shots varying between 1000 and 10,000, depending on the ablation rate at the specific fluence employed. At the lowest fluences, instead, a number of shots as high as 100,000 must be employed in order to get films 10–50 nm thick.

By measuring the film thickness at different points corresponding to different emission angles ϑ from the normal to the target (see inset in Fig. 6), we estimated the angular distribution of the emitted material.

In Fig. 6 the thickness of the deposited films (normalized to the maximum value for each substrate) vs ϑ is reported for three laser fluences within the three observed regions of ablation rate. The shift of the maximum of the distribution to larger emission angle is due to the particular geometry adopted.

For the two highest fluences the angular dependence of the thickness is very narrow, and within the experimental error, the two curves are equal. The maximum is close to 0° and the FWHM is about 15°. This shape could be fitted by assuming a $\cos^n \vartheta$ law of emission with $n \sim 35$. This is the typical angular distribution of the emitted plasma plume [10].

For the lowest fluency instead, a broad maximum at $\vartheta \sim 10°$ is seen and a FWHM greater than 35° is estimated. Although this distribution is not the expected $\cos \vartheta$ law, it suggests that pure thermal evaporation took place; the deviation from the theoretical law could be ascribed to the

roughness of the evaporating source. The formation of cones, typical of multishot irradiations [11], could infact shield the substrate from particles emitted at large angles.

4. CONCLUSIONS

In conclusion, we have shown that ablation of crystalline 6*H*–α SiC with XeCl 15-ns laser pulses is characterized by two well-defined fluence thresholds: at $1\ J \cdot cm^{-2}$, which is also the surface melting threshold, pure thermal evaporation produces an emission of about $10^{-1}\ Å \cdot pulse^{-1}$; it increases up to $\sim 1 Å \cdot pulse^{-1}$ with increasing fluence up to $1.6\ J \cdot cm^{-2}$. This is the onset of a different mechanism, for which the ablation rate is rapidly enhanced to $600\ Å \cdot pulse^{-1}$ when the fluence is increased to $2.2\ J \cdot cm^{-2}$. A saturation effect, probably due to plasma shielding of the laser light, is observed at higher fluence.

The process can be qualitatively described as the thermal evaporation of a hot liquid. When the evaporation rate and the laser fluence are high enough to raise the temperature and the pressure up to the critical point, an almost-instantaneous transition to a highly compressed vapor phase occurs. This interpretation, supported by heat flow and pressure calculations, explains the low-fluence regime up to the threshold for plasma formation.

REFERENCES

1. M. Balooch, R. J. Tench, W. J. Siekhans, R. J. Allen, A. L. Connor, and D. R. Holander, *Appl. Phys. Lett.* **57**:1540 (1990).
2. T. Zehnder, A. Blatter, and A. Bachli, *Thin Solid Films* **241**:138 (1994).
3. L. Rimai, R. Ager, E. M. Logothetis, W. H. Weber, and J. Hangus, *Appl. Phys. lett.* **59**:2267 (1991).
4. J. A. Powell, D. J. Larkin, L. G. Matus, W. J. Choike, J. L. Brodshow, L. Menderson, M. Yoganathan, J. Yang, and P. Pirouz, *Appl. Phys. Lett.* **56**:1942 (1990).
5. P. Baeri and S. U. Campisano, *Laser Annealing of Semiconductors* (Academic Press, New York, 1982), pp. 75–108.
6. JANAF Thermochemical Tables, *J. Phys. Chem. Ref. Data* **14**:636 (1985).
7. R. W. Olesinski and G. J. Abbaschian, *Bull. Alloy Phase Diagrams* **5**:486 (1984).
8. L. Kaufman, *CALPHAD* **3**:45 (1979).
9. M. M. Martinyuk, *Sov. Phys. Tech. Phys.* **21**:430 (1976); M. M. Martynyuk, *Radio Eng. Electron. Phys.* **25**:100 (1980).
10. K. L. Saenger, *J. Appl. Phys.* **70**:5629 (1991).
11. J. E. Rothemberg and R. Kelly, *Nucl. Instr. Meth. Phys. Res.* **B1**:291 (1984).